Secondary Through-Space Interactions Promoted White-Light Emission of Clusteroluminogens with Isolated Phenyl Rings

Jianyu Zhang,[†#] Parvej Alam,[†#] Siwei Zhang,[†#] Hanchen Shen,[†] Lianrui Hu,[†] Herman H. Y. Sung,[†] Ian D. Williams,[†] Jianwei Sun,[†] Jacky W. Y. Lam,*[†] Haoke Zhang,*[‡§⊥] and Ben Zhong Tang*[†‖]

[†]Department of Chemistry, Hong Kong Branch of Chinese National Engineering Research Center for Tissue Restoration and Reconstruction, and Guangdong-Hong Kong-Macau Joint Laboratory of Optoelectronic and Magnetic Functional Materials, The Hong Kong University of Science and Technology, Clear Water Bay, Kowloon, Hong Kong 999077, China

[‡]MOE Key Laboratory of Macromolecular Synthesis and Functionalization, Department of Polymer Science and Engineering, Zhejiang University, Hangzhou 310027, China

[§]ZJU-Hangzhou Global Scientific and Technological Innovation Center, Hangzhou 311215, China

[⊥]Guangdong Provincial Key Laboratory of Luminescence from Molecular Aggregates, South China University of Technology, Guangzhou 510640, China

[‖]Shenzhen Institute of Aggregate Science and Technology, School of Science and Engineering, The Chinese University of Hong Kong, Shenzhen, 2001 Longxiang Boulevard, Longgang District, Shenzhen City, Guangdong, 518172, China

[#]J.Zhang, P.Alam and S.Zhang contributed equally to this work.

Abstract: Clusteroluminogens (CLgens) refer to some non-conjugated molecules that show visible light due to the formation of aggregates and unique electronic properties with through-space interactions (TSI). While mature and systematic theories of molecular photophysics have been developed to study conventional conjugated chromophores, it is still challenging to endow CLgens with designed photophysical properties by manipulating TSI. Herein, three CLgens with non-conjugated donor-acceptor structures and different halide substituents with secondary through-space interactions are designed and synthesized. These molecules show multiple emissions and even white-light emission in the crystalline state and the intensity ratio of these multiple emission peaks is easily manipulated by changing the halide atom and excitation wavelength. Experimental and theoretical results successfully disclose the electronic nature of these multiple emissions: through-space conjugation for short-wavelength fluorescence, through-space charge transfer based on secondary TSI for long-wavelength fluorescence, and room-temperature phosphorescence. The introduction of secondary TSI to CLgens not only enriches their varieties of photophysical properties but also inspires the establishment of novel aggregate photophysics for clusteroluminescence.

Keywords: Through-space interactions, clusteroluminogens, multiple emissions, aggregates, clusteroluminescence

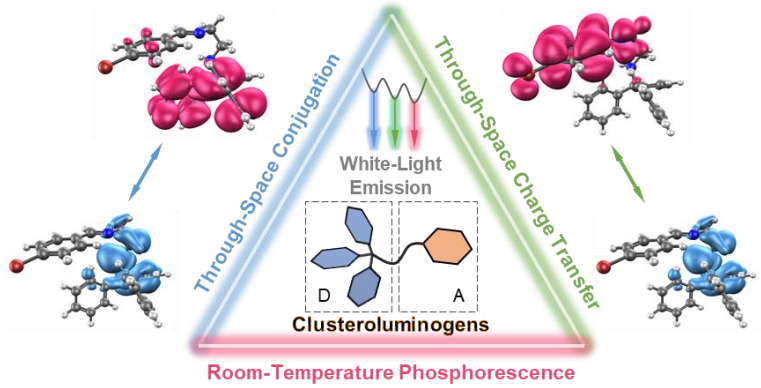

Introduction

Luminescent material not only brightens our life but also leads to far-reaching revolutions in many high-tech areas such as encryption, imaging, and sensor.[1, 2] In the past decades, molecular photophysics based on through-bond conjugation (TBC) has been established to guide the design of efficient and multifunctional organic luminophores, and structures with extended π-conjugation are recognized as the prerequisite for high luminescence performance.[3-5] However, some non-conjugated molecules have attracted great attention recently due to their ability to emit visible light in the aggregate state.[6-8] For example, non-conjugated and nonaromatic poly(amido amine) dendrimers and succinimide derivatives show strong blue and green emission in the cluster state, respectively.[9-11] This non-conventional luminescence is termed as clusteroluminescence (CL) and the luminophores with such property are known as clusteroluminogens (CLgens).[12, 13] Compared with traditional luminophores with conjugated aromatic rings, CLgens possess better flexibility, processability and biocompatibility, and are promising luminescent materials for biological applications.

However, different from traditional conjugated luminophores, the TBC-based theories sometimes fail to explain the photophysical behaviors of CLgens. Thus, there is an urgent need to build new photophysical theories for CL.[14] Previous reports indicate that the through-space interaction (TSI) or electron coupling/delocalization of spatially separated units play an essential role in the visible emission of non-conjugated CLgens.[15] For instance, 1,1,2,2-tetraphenylethane, in which its phenyl rings are isolated from each other by saturated carbons, shows sky blue emission in the solid state due to the excited-state electron overlapping of the phenyl rings.[16] Tang et al. also demonstrated the possibility to regulate TSI by introducing electron-donating and withdrawing groups to not only adjust the electron density but also affect the rigidity of excited-state geometry.[17] Although several achievements have been received in TSI-related studies, it is still a big challenge to improve the photophysical performance of CLgens by manipulating the TSI at the molecular level.

In contrast, many effective strategies have been developed to modify the electronic structures of conjugated chromophores according to the theory of TBC, such as the excited-state intramolecular proton transfer,[18] twisted intramolecular charge transfer,[19, 20] and photoinduced electron transfer.[21] Because of the diversified electronic structures and properties, it is easy to fabricate single-molecule white-light emission (WLE) in conjugated molecules via multiple emissions.[22-24] As shown in Figure 1a, the incorporation of locally excited state, charge transfer state, and room-temperature phosphorescence (RTP) is a typical mechanism for multiple

emissions from conjugated chromophores with moderate donor-acceptor structures.[25-28] However, the rigid structures of these molecules makes it difficult to regulate the intensity ratio of these multiple emissions. On the other hand, the non-conjugated and flexible structures of CLgens endow them with sensitive response to internal and external stimuli, which is beneficial to the generation of multiple emissions and WLE. Unfortunately, it is still a thorny issue to realize WLE in CLgens by manipulating their TSI.

In this work, we proposed a novel strategy to achieve multiple emissions and WLE from single-component CLgens with totally isolated phenyl rings (Figure 1b, c). Three compounds, named TPMI-X (X = Cl, Br and I), were synthesized and fully characterized based on triphenylmethanamine (TPMA) and halogen-substituted phenylmethanimine (PMI-X) (Scheme S1 and Figures S1−S9 in the Supporting Information). Photophysical measurements revealed two fluorescent emission peaks and RTP in the crystalline state, meanwhile, the intensity of these multiple peaks can be manipulated by both the internal heavy-atom effect and external excitation energy. Additionally, theoretical calculations indicated the important role of through-space conjugation (TSC) of TPMA and secondary TSI, and the through-space charge transfer (TSCT) of TPMA and PMI-X in producing WLE. Thus, this work not only provides a general strategy to achieve single-molecule WLE from unconventional CLgens but also enriches the photophysical behaviors and mechanistic understanding of CL and TSI.

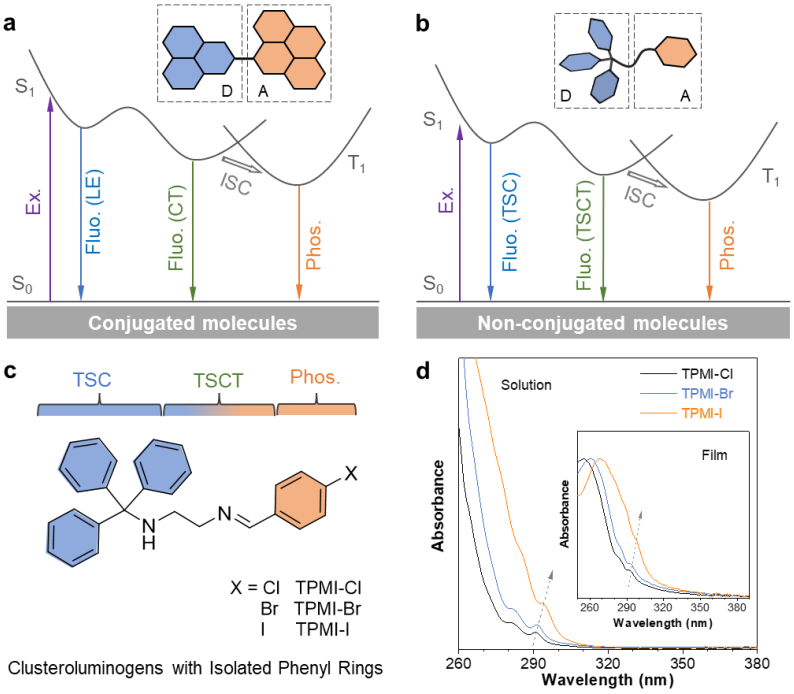

Figure 1. (a) A typical mechanism of multiple emission from organic molecules with large conjugated structures. (b) Proposed multiple emissions from non-conjugated molecules with isolated phenyl rings. (c) Designed molecules based on triphenylmethanamine and phenylmethanimine groups connected by flexible ethyl chain. (d) Absorption spectra of TPMI-Cl, TPMI-Br, and TPMI-I in THF solution and solid film, respectively. Ex. = excitation, Fluo. = fluorescence, Phos. = phosphorescence, LE = locally excited, CT = charge transfer, TSC = through-space conjugation, TSCT = through-space charge transfer, ISC = intersystem crossing, D = electron donor, A = electron acceptor.

Results and Discussion

Photophysical properties. The absorption spectra of the newly synthesized compounds were first measured (Figure 1d). All the molecules exhibited peak maximums with a wavelength of shorter than 300 nm in both THF solution and solid state, which were assigned to the absorption of phenylmethanimine group and isolated phenyl rings. This result suggested that non-conjugated nature of the molecules. On the other hand, no photoluminescence (PL) signals were detected in their pure THF solutions and even THF/H_2O (9:1, *v*/*v*) mixtures where aggregates were formed (Figures S10 and S11). This was presumably due to the flexible structure of TPMI-X, where the vigorous molecular motion could not be effectively restricted even in the aggregate state. Bulk crystals of the molecules were easily obtained through recrystallization from their water/ethanol mixtures and were highly emissive under 365 nm UV irrdiation, suggesting their characteristics of aggregation-induced emission (AIE).[29-31] Figures 2 and S12 showed their PL spectra in the crystalline state. All the spectra showed two peaks in the visible range, where their intensity was excitation dependent. For TPMI-Cl, while the peak at around 400 nm was dominant, another low-intensity shoulder peak was located at 490 nm. The nature of these two emissions was assigned to fluorescence as suggested by their nanosecond lifetimes (Figure S13), and the lifetime at 490 nm was longer than that at 400 nm. The TPMI-Cl crystal exhibited blue-white emission with an absolute quantum yield (QY) of 34.8% at an excitation wavelength (λ_{ex}) of 370 nm. When the halogen atom was replaced by different elements from Cl to Br and I, the long-wavelength peak gradually intensified and became dominant, and its position also red-shifted to 500 (TPMI-Br) and 506 nm (TPMI-I), respectively (Figure 2b, c). Interestingly, TPMI-Br showed a perfect emission balance and demonstrated white-light emission with a QY of 28.3% at λ_{ex} = 370 nm. The long-wavelength emission was dominant in TPMI-I and it overall showed green-white emission with a QY of 14.6%. It is noteworthy that the intensity ratio (I_L/I_S) of the long- (I_L) and short-wavelength emission (I_S) of each compound decreased progressively along with the increased λ_{ex} (Figure 2d). This was explained by their excitation spectra, where the long-wavelength emission was much strongly dependent on λ_{ex} than the short-wavelength one, although two excitation spectra were strongly mixed due to the vibronic coupling (Figure S14). Besides, at the same λ_{ex}, the ratio of I_L/I_S decreased in the order from TPMI-I to TPMI-Br and then to TPMI-Cl. After grinding the bulk crystals of the molecules, amorphous powders were formed and their PL spectra were recorded and shown in Figure S15. All the spectra displayed broad peaks where the short- and long-wavelength emission were mixed. The associated QYs were much lower than those in the crystalline state and changed slightly at different λ_{ex}. These results indicated that their PL performance was closely related to the intra-/intermolecular interactions in the crystalline state and the halide substituents.

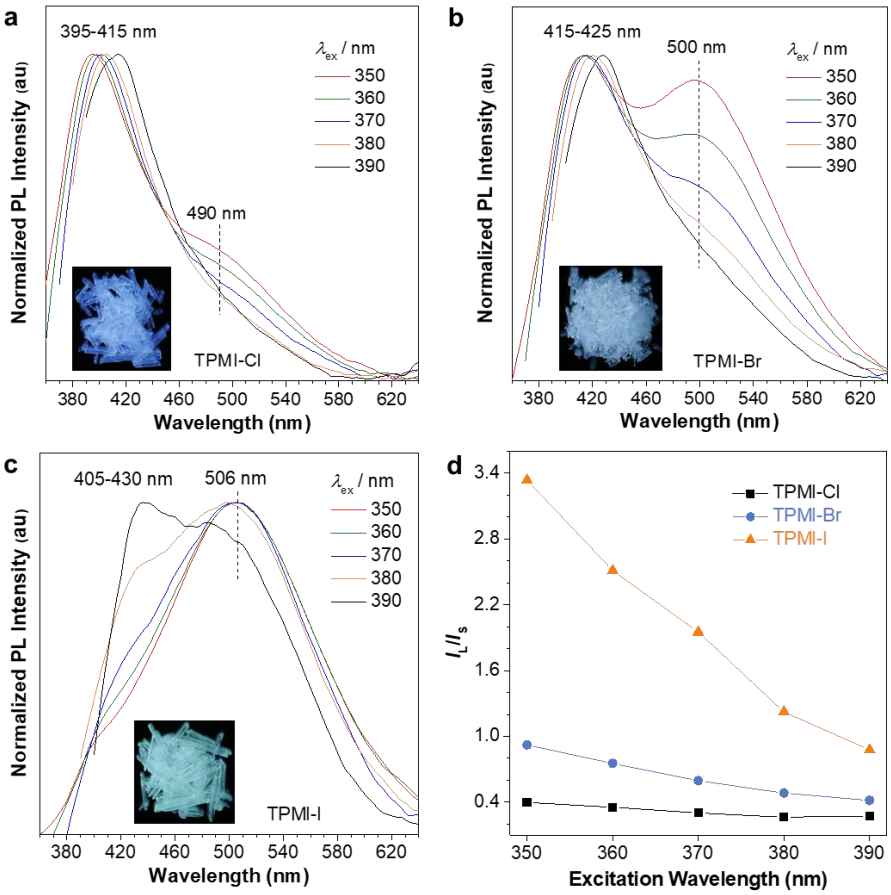

Figure 2. Normalized photoluminescence (PL) spectra of (a) TPMI-Cl, (b) TPMI-Br, and (c) TPMI-I in the crystalline state at different excitation wavelengths; Inset: photo of the crystals taken under the 365 nm UV irradiation from a hand-held UV lamp. λ_{ex} = excitation wavelength. (d) Plots of relative PL (I_L/I_S) versus the excitation wavelength, where I_L = intensity maximum of the long-wavelength emission and I_S = intensity maximum of the short-wavelength emission.

Additionally, RTP was also observed from the three molecules as depictyed in Figure 3. All the molecules exhibited similar RTP peaks at around 560-600 nm, although their fluorescent properties were different. The RTP lifetime was 24 ms in TPMI-Cl, which was shortened to 17 ms in TPMI-Br and 5.1 ms in TPMI-I, due to the law of heavy-atom effect.[28, 32, 33] At the cryogenic temperature of 77 K, the phosphorescent emission became stronger, shifted to the bluer region and showed a longer lifetime (Figure S16). Thus, the above results verified the ability of the present compounds as CLgens with multiple emissions and even WLE, despite their non-conjugated structures.

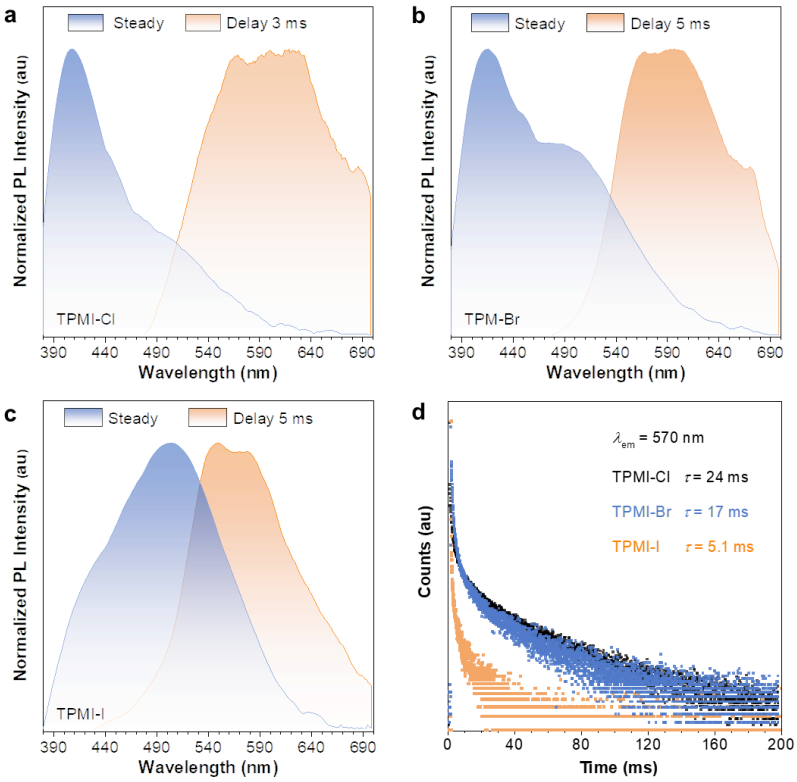

Figure 3. Normalized steady and delayed photoluminescence (PL) spectra of (a) TPMI-Cl, (b) TPMI-Br, and (c) TPMI-I in the crystalline state. (d) Time-resolved PL decay curves of the compounds at emission maximum (λ_{em}) of 570 nm. λ_{ex} = 365 nm.

Secondary through-space interactions. To disclose the mechanism and origin of the unusual multiple emissions of the present CLgens, two model compounds, namely, *N*-methyl-TPMA and halogen-substituted *N*-methyl-phenylmethanimine (*N*-methyl-PMI-X, X = Cl, Br and I), were synthesized and characterized (Scheme S2). As expected, the UV spectrum of *N*-methyl-TPMA showed an maximum at 264 nm which corresponded to the absorption of isolated phenyl rings (Figure S17). Interestingly, *N*-methyl-TPMA showed visible emission of 445 nm. The corresponding excitation maximum was located at 366 nm, which was ascribed to the TSC of the isolated phenyl rings and such interaction could be directly visualized from the natural transition orbitals (NTO) with spatial electron communication.[17] As shown in Figure S17c, the emission wavelength was very close to the short-wavelength emission of the three CLgens. On the other hand, *N*-methyl-PMI-X showed maximum absorption and emission at around 290 and 300 nm, respectively, and the NTO analysis suggested a (π,π*) transition (Figure S18). However, the emission wavelength was much shorter than that of TPMI-X. Thus, the above results indicated that the short-wavelength emission of TPMI-X should origin from the TSC of the TPMA moiety.

To further unveil the electronic nature of these emission peaks in TPMI-X, TPMI-Br was selected as an example to investigate the photophysical mechanism with the help of theoretical calculation. From the NTO analysis of TPMI-Br in the excited state, it was obvious that the hole and electron were mainly distributed on the TPMA moiety and the hole-electron distribution was almost the same as that of TPMA showing TSC (left panel in Figure 4a and Figure S17). Besides, the calculated energy gap (E_{em} (cal.)) of 3.43 eV was comparable to that of the short-wavelength

emission at 410 nm (E_{em} (exp.) = 3.00 eV). The combined experimental and theoretical results supported the TSC as the origin of the short-wavelength emission of TPMI-Br.

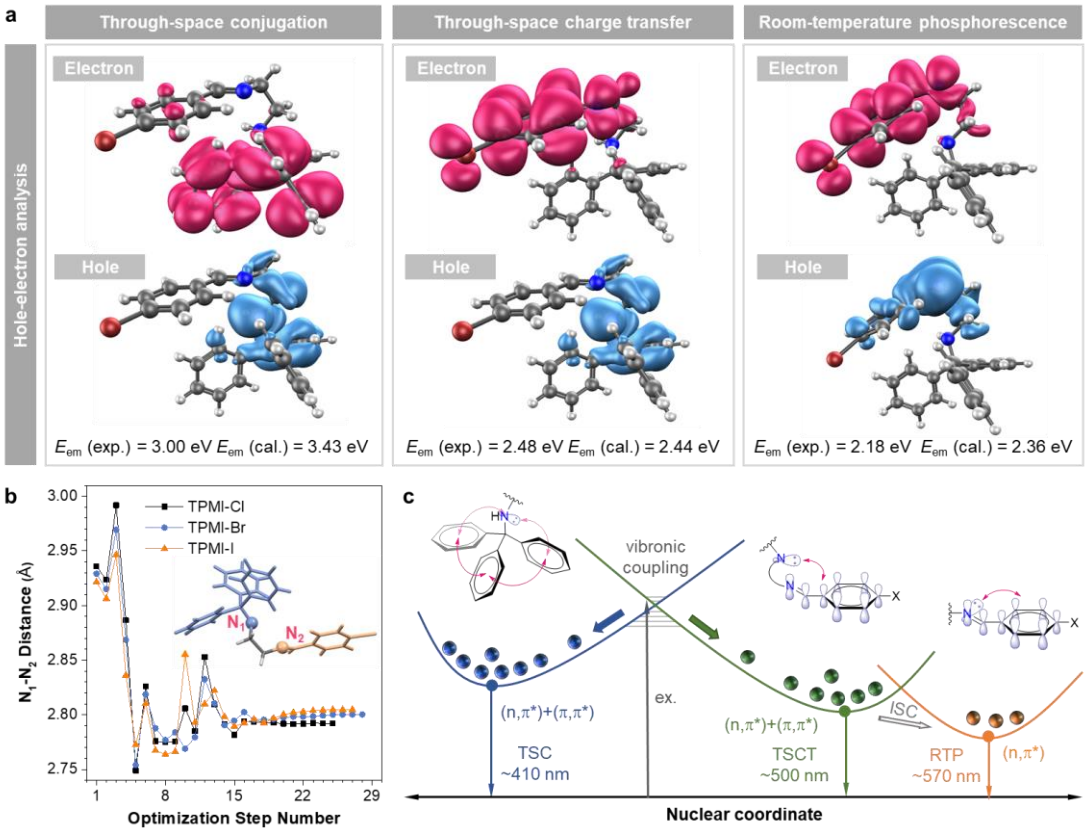

Figure 4. Proposed mechanism of multiple emissions of designed clusteroluminogens. (a) Natural transition orbitals of TPMI-Br based on the optimized corresponding geometries calculated at B3LYP-D3/Def2-SVP level of Gaussian 09 program. (b) Plot of N_1−N_2 distance versus optimization steps from the ground state to the excited TSCT state. Inset: structure of the designed clusteroluminogens with two highlighted N atoms. (c) Potential energy surface and electronic behaviors of the designed clusteroluminogens to realize multiple emissions. TSC = through-space conjugation, TSCT = through-space charge transfer, RTP = room-temperature phosphorescence.

In consideration of the non-conjugated donor-acceptor structure of TPMI-Br, the charge transfer (CT) process of separated TPMA and PMI-Br moieties was further investigated. As shown in the middle panel of Figure 4a, another low-lying excited state with CT feature was mapped where the hole and electron were distributed on the TPMA and PMI-Br parts, respectively. Meanwhile, the calculated energy gap of 2.44 eV was almost the same as that of the long-wavelength emission at 500 nm (E_{em} (exp.) = 2.48 eV), suggesting the accurate simulation of geometry and electronic transition behavior. Since the donor (TPMA) and acceptor (PMI-Br) units were separated by a flexible and saturated ethyl linker, this transition was regarded as another important through-space behavior known as through-space charge transfer (TSCT). It is noteworthy that, different from the traditional TSCT effect which was caused by the interaction of TBC-based donor and acceptor units,[34-37] the TSCT in TPMI-Br is based on the non-conjugated donor with TSC. This special interaction was termed as secondary TSI where the TSCT was generated from a TSC-based CLgens, which was responsible for the long-wavelength fluorescence

of TPMI-Br and also TPMI-Cl and TPMI-I.

Since the TSCT effect was not reflected in the absorption spectra (Figure 1d), the excited-state intramolecular motion should play another critical role to facilitate the TSCT transition.[38, 39] Accordingly, the distance between two nitrogen atoms (N_1-N_2) and the dihedral angle of the two separated parts ($\angle N_1$-C_1-C_2-N_2) were tracked along with the optimization process from the optimized ground state to the excited TSCT state. Figure 4b showed that the N_1−N_2 distance became shorter from the ground-state geometry of 2.93 Å to the excited-state geometry of 2.80 Å, and the dihedral angle also decreased from 65° to 50° (Figure S19). These variations indicated that the electron overlapping of the two separated groups was enhanced in the excited state, which formed an efficient (n,π*) transition channel for TSCT. TPMI-Cl and TPMI-I displayed similar hole-electron distribution and geometry change (Figures S20 and S21 and Table S1), suggesting that the secondary TSI played a crucial role to realize the long-wavelength fluorescent emission.

Besides, the origin of RTP was also investigated. Both the triplet spin density and hole-electron distribution of TPMI-Br indicated that its phosphorescence was aroused by the (n,π*) transition of PMI-Br moiety (right panel in Figure 4a, and Figure S22). Meanwhile, the calculated triplet-state energy gap of 2.36 eV was close to the long-wavelength phosphorescence at 570 nm (E_{em} (exp.) = 2.18 eV). However, the triplet-state (n,π*) transition of TPMI-Br was different from that of *N*-methyl-PMI-Br with triplet (π,π*) transition (Figure S23). This might be due to the ethyl chain of TPMI-Br which ruined its planarity and altered the energy level of n and π orbitals.

According to the above results, a comprehensive picture of multiple emissions of the CLgens was drawn and clarified (Figure 4c). After excitation from the ground state, two relaxtion pathways, namely TSC and TSCT states, were feasible due to their overlapped excitation spectra and strong vibronic coupling (Figure S14). The TSC state was related to the spatial electron communication of the three isolated phenyl rings in TPMA moiety and showed blue emission at around 410 nm. On the other hand, the TSCT state relies on the (n,π*) transition of the two separated parts which formed secondary TSI via excited-state intramolecular motion and to give long-wavelength green emission at 500 nm. Due to the prescence of halogen atoms and enhanced intersystem crossing, the RTP from the PMI-X moiety of TPMI-Cl, TPMI-Br and TPMI-I at around 570 nm was also detected.

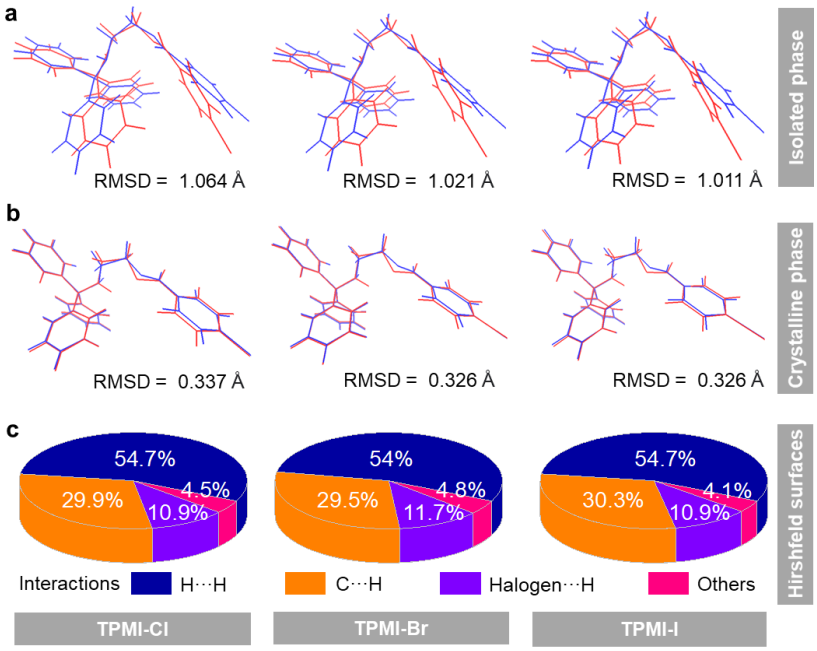

Figure 5. Overlap of the optimized ground-state geometry (blue color) and singlet TSCT geometry (red color) of TPMI-X in the (a) isolated phase and (b) crystalline phase. The root-mean-square deviation (RMSD) of atomic positions was calculated to evaluate the strength of intramolecular motions in two different phases. (c) Hirshfeld surface analysis and proportions of intermolecular C···H, H···H, halogen···H and other interactions to the total intermolecular interactions based on their crystal structures.

Clusteroluminescence. To better understand the different photophysical behaviors of TPMI-X in the isolated and crystalline states, their molecular motions in the two states were also investigated. As expected, all the molecules showed strong intramolecular motions in the isolated phase, as evidenced by the large value of root-mean-square deviation (RMSD) of atomic positions which was more than 1 Å between the ground state (molecule with blue color) and excited TSCT state (molecule with red color) (Figure 5a). The poorly overlapped molecular geometries also demonstrated their flexible structure and vigerous intramolecular motions, to result in totally quenched emission even in the aggregate state. However, in the crystalline state, the intramolecular motions were restricted to a confined level with a small RMSD value of 0.3 Å, which suggested the restriction of intramolecular motion (RIM) as the mechanism for the AIE effect and crystalline-state light emission of the CLgens (Figure 5b).[40-42] The RIM mechanim simultaneously inhibited the nonradiative decay and promoted the formation of secondary TSI and long-wavelength emission from the TSCT state. Besides, the strength of intersystem crossing (ISC) of TPMI-X was also evaluated (Figure S24). They all showed small energy gaps between the singlet and triplet states and comparatively large constants of spin-orbital coupling in both the isolated and crystalline states. These results indicated that crystalline environment and RIM exerted no influence on the TSC efficiency but suppressed the nonradiative decay to finally promot RTP and multiple emissions.

In addition, single-crystal X-ray diffraction technique was utilized to investigate the crystal structures to disclose their varied in photophysical properties (Table S2). All the molecules exhibited similar head-to-tail arrangement where each halogen atom formed two halogen···H

bonds with the urrounding molecule (Figure S25-S27). Hirshfeld surface analysis based on the crystal structures was performed to quantitatively evaluate their intermolecular interactions.[43] As shown in Figures 5c and S28, these weak intermolecular C···H, H···H, and halogen···H interactions accounted for more than 95% to total intermolecular interactions, and mainly contributed to the RIM mechanism. Besides, the results also verified that multiple emissions were originated from the intramolecular photophysical processes instead of intermolecular rigidification.

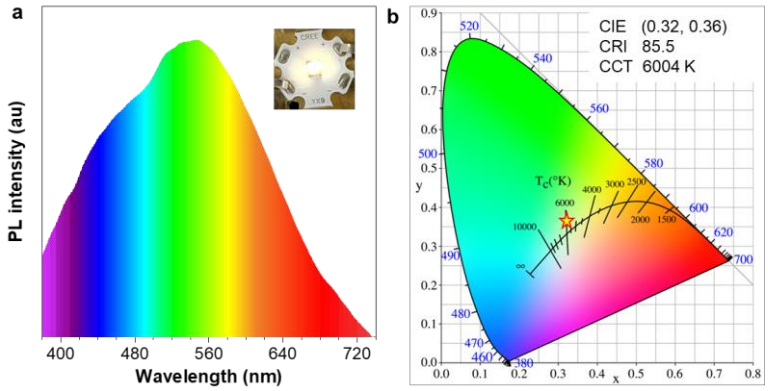

Figure 6. (a) The electroluminescence spectra and digital photo of fabricated white OLED by coating microcrystals of TPMI-Br and epoxy resin glue on a commercial UV chip. (b) The Commission Internationale de L'Eclairage (CIE) chromaticity coordinate of the fabricated white OLED. CRI = color rendering index, CCT = correlated color temperature.

White OLED. In light of the particular multiple emission of the three CLgens and their excellent thermal stability (Figure S29), a prototype organic light-emitting diode (OLED) was fabricated by coating a mixture of TPMI-Br microcrystals and epoxy resin glue on a commercial UV chip (Figure 6). Within the current range considered, the fabricated OLED displayed bright white-light emission with a Commission Internationale de L'Eclairage (CIE) chromaticity coordinate of (0.32, 0.36), which was close to the value of standard white light. The electroluminescence spectrum fitted well with the PL spectrum of TPMI-Br crystal. Besides, the color of the fabricated OLED exhibited high quality with a color rendering index of 85.5 and correlated color temperature of 6004 K, suggesting its potential for daylight illumination and displaying. Similarly, the fabricated OLEDs based on TPMI-Cl and TPMI-Ishowed similar electroluminescence with cold-white and daylight color, respectively (Figures S30 and S31).

Conclusion

In this work, three non-conjugated CLgens, namely TPMI-X (X = Cl, Br and I), based on flexible ethyl-linked TPMA (donor) and PMI-X (acceptor) were synthesized, and their photophysical properties were systematically investigated. All the molecules displayed multiple emissions consisting of two fluorescence components and one RTP unit in the crystalline state, and the highest absolute quantum yield of 34.8%. The intensity ratio of these multiple peaks was easily manipulated by changing the halide substituent and external excitation wavelength, demonstrating their tremendous potential in producing white-light emisison. Theoretical calculation and crystal structure analysis proved that the short-wavelength fluorescence was stemmed from the TSC of

TPMA moiety. Because of the non-conjugated donor-acceptor structure, the peculiar intramolecular TSCT interaction as secondary TSI was formed between TPMA and PMI-X to promote the long-wavelength fluorescence. Halogen-atom assisted RTP was observed as the third emission peak. In addition, the multiple intermolecular interactions provided a rigid environment to restrict the intramolecular motions of the flexible structures and stabilize the excited-state geometries, to lead to the highly efficient multiple emissions. A prototype white OLED based on TPMI-I was fabricated with a CIE coordinate of (0.32, 0.36) and CCT value of 6004 K, indicating its excellent potential for daylight illumination and display.

We innovatively introduced the concept of secondary through-space interactions of CLgens. Similar to the important role of secondary structure in protein bioactivity, the through-space charge transfer based on non-conjugated moiety with TSC endows CLgens with versatile and controllable photophysical behaviors, which will be a promising and significant theory of aggregate photophysics for non-conjugated CLgens. It is anticipated that, because of secondary TSI, clusteroluminescence will become an influential luminescent form not only in fundamental research but also for the cutting edge of technology development and application.

Acknowledgments

This work was supported by the National Natural Science Foundation of China Grant (21788102), the Research Grants Council of Hong Kong (16304819, 16307020, C6014-20W, N_HKUST609/19 and 16305320), the Innovation and Technology Commission (ITC-CNERC14SC01), and the Natural Science Foundation of Guangdong Province (2019B121205002 and 2019B030301003). H. Z thanks to the support from the Fundamental Research Funds for the Central Universities (2021QNA4032) and the Open Fund of Guangdong Provincial Key Laboratory of Luminescence from Molecular Aggregates, and the South China University of Technology (2019B030301003).

Reference

(1) Al-Amri, M. D.; El-Gomati, M. M.; Zubairy, M. S. *Optics in Our Time*; Springer Nature, 2016; pp 4−24.

(2) Yang, J.; Fang, M.; Li, Z. Organic Luminescent Materials: The Concentration on Aggregates from Aggregation-Induced Emission. *Aggregate* **2020**, *1*, 6-18.

(3) Yamaguchi, Y.; Matsubara, Y.; Ochi, T.; Wakamiya, T.; Yoshida, Z. How the π Conjugation Length Affects the Fluorescence Emission Efficiency. *J. Am. Chem. Soc.* **2008**, *130*, 13867-13869.

(4) Yu, T.; Liu, L.; Xie, Z.; Ma, Y. Progress in Small-Molecule Luminescent Materials for Organic Light-Emitting Diodes. *Sci. China Chem.* **2015**, *58*, 907-915.

(5) Xu, S.; Duan, Y.; Liu, B. Precise Molecular Design for High-Performance Luminogens with Aggregation-Induced Emission. *Adv Mater* **2020**, *32*, 1903530.

(6) Tang, S.; Yang, T.; Zhao, Z.; Zhu, T.; Zhang, Q.; Hou, W.; Yuan, W. Z. Nonconventional Luminophores: Characteristics, Advancements and Perspectives. *Chem. Soc. Rev.* **2021**, *50*, 12616-12655.

(7) Yang, S.-Y.; Qu, Y.-K.; Liao, L.-S.; Jiang, Z.-Q.; Lee, S.-T. Research Progress of Intramolecular π-Stacked Small Molecules for Device Applications. *Adv. Mater.* **2021**. DOI:

10.1002/adma.202104125.
(8) Zhang, Z.; Zhang, H.; Kang, M.; Li, N.; Wang, D.; Tang, B. Z. Oxygen and Sulfur-Based Pure N-Electron Dendrimeric Systems: Generation-Dependent Clusteroluminescence Towards Multicolor Cell Imaging and Molecular Ruler. *Sci. China Chem.* **2021**, *64*, 1990-1998.
(9) Pucci, A.; Rausa, R.; Ciardelli, F. Aggregation-Induced Luminescence of Polyisobutene Succinic Anhydrides and Imides. *Macromol. Chem. Phys.* **2008**, *209*, 900-906.
(10) He, B.; Zhang, J.; Zhang, J.; Zhang, H.; Wu, X.; Chen, X.; Kei, K. H. S.; Qin, A.; Sung, H. H. Y.; Lam, J. W. Y.; Tang, B. Z. Clusteroluminescence from Cluster Excitons in Small Heterocyclics Free of Aromatic Rings. *Adv. Sci.* **2021**, *8*, 2004299.
(11) Wang, R.; Yuan, W.; Zhu, X. Aggregation-Induced Emission of Non-Conjugated Poly(Amido Amine)S: Discovering, Luminescent Mechanism Understanding and Bioapplication. *Chin. J. Polym. Sci.* **2015**, *33*, 680-687.
(12) Zhang, H.; Zhao, Z.; McGonigal, P. R.; Ye, R.; Liu, S.; Lam, J. W. Y.; Kwok, R. T. K.; Yuan, W. Z.; Xie, J.; Rogach, A. L.; Tang, B. Z. Clusterization-Triggered Emission: Uncommon Luminescence from Common Materials. *Mater. Today* **2019**, *32*, 275-292.
(13) Wang, Z.; Zhang, H.; Li, S.; Lei, D.; Tang, B. Z.; Ye, R. Recent Advances in Clusteroluminescence. *Top. Curr. Chem.* **2021**, *379*, 14.
(14) Hoffmann, R. Interaction of Orbitals through Space and through Bonds. *Acc. Chem. Res.* **1971**, *4*, 1-9.
(15) Zhang, H.; Tang, B. Z. Through-Space Interactions in Clusteroluminescence. *JACS Au* **2021**, *1*, 1805-1814.
(16) Zhang, H.; Zheng, X.; Xie, N.; He, Z.; Liu, J.; Leung, N. L. C.; Niu, Y.; Huang, X.; Wong, K. S.; Kwok, R. T. K.; Sung, H. H. Y.; Williams, I. D.; Qin, A.; Lam, J. W. Y.; Tang, B. Z. Why Do Simple Molecules with "Isolated" Phenyl Rings Emit Visible Light? *J. Am. Chem. Soc.* **2017**, *139*, 16264-16272.
(17) Zhang, J.; Hu, L.; Zhang, K.; Liu, J.; Li, X.; Wang, H.; Wang, Z.; Sung, H. H. Y.; Williams, I. D.; Zeng, Z.; Lam, J. W. Y.; Zhang, H.; Tang, B. Z. How to Manipulate through-Space Conjugation and Clusteroluminescence of Simple Aiegens with Isolated Phenyl Rings. *J. Am. Chem. Soc.* **2021**, *143*, 9565-9574.
(18) Tang, K.-C.; Chang, M.-J.; Lin, T.-Y.; Pan, H.-A.; Fang, T.-C.; Chen, K.-Y.; Hung, W.-Y.; Hsu, Y.-H.; Chou, P.-T. Fine Tuning the Energetics of Excited-State Intramolecular Proton Transfer (ESIPT): White Light Generation in a Single ESIPT System. *J. Am. Chem. Soc.* **2011**, *133*, 17738-17745.
(19) Tu, Y.; Yu, Y.; Xiao, D.; Liu, J.; Zhao, Z.; Liu, Z.; Lam, J. W. Y.; Tang, B. Z. An Intelligent Aiegen with Nonmonotonic Multiresponses to Multistimuli. *Adv. Sci.* **2020**, *7*, 2001845.
(20) Xu, Z.; Wang, C.; Qiao, Q.; Chi, W.; Chen, J.; Liu, W.; Tan, D.; McKechnie, S.; Lyu, D.; Jiang, X.-F.; Zhou, W.; Xu, N.; Zhang, Q.; Liu, X. Quantitative Design of Bright Fluorophores and AIEgens via the Accurate Prediction of Twisted Intramolecular Charge Transfer (TICT). *Angew. Chem. Int. Ed.* **2020**, *59*, 10160-10172.
(21) Chi, W.; Chen, J.; Liu, W.; Wang, C.; Qi, Q.; Qiao, Q.; Tan, T. M.; Xiong, K.; Liu, X.; Kang, K.; Chang, Y. T.; Xu, Z.; Liu, X. A General Descriptor ΔE Enables the Quantitative Development of Luminescent Materials Based on Photoinduced Electron Transfer. *J. Am. Chem. Soc.* **2020**, *142*, 6777-6785.
(22) Kukhta, N. A.; Bryce, M. R. Dual Emission in Purely Organic Materials for Optoelectronic Applications. *Mater. Horiz.* **2020**, *8*, 33-55.

(23) Chen, Z.; Ho, C.-L.; Wang, L.; Wong, W.-Y. Single-Molecular White-Light Emitters and Their Potential Woled Applications. *Adv. Mater.* **2020**, *32*, 1903269.

(24) Zhao, X.; Alam, P.; Zhang, J.; Lin, S.; Peng, Q.; Zhang, J.; Liang, G.; Chen, S.; Zhang, J.; Sung, H. H. Y.; Lam, J. W. Y.; Williams, I. D.; Gu, X.; Zhao, Z.; Tang, B. Z. Metallophilicity-Induced Clusterization: Single-Component White-Light Clusteroluminescence with Stimulus Response. *CCS Chem.* **2021**, *3*, 3039-3049.

(25) Tu, D.; Leong, P.; Guo, S.; Yan, H.; Lu, C.; Zhao, Q. Highly Emissive Organic Single-Molecule White Emitters by Engineering *o*-Carborane-Based Luminophores. *Angew. Chem. Int. Ed.* **2017**, *56*, 11370-11374.

(26) Wu, Y. H.; Xiao, H.; Chen, B.; Weiss, R. G.; Chen, Y. Z.; Tung, C. H.; Wu, L. Z. Multiple-State Emissions from Neat, Single-Component Molecular Solids: Suppression of Kasha's Rule. *Angew. Chem. Int. Ed.* **2020**, *59*, 10173-10178.

(27) Weng, T.; Baryshnikov, G.; Deng, C.; Li, X.; Wu, B.; Wu, H.; Agren, H.; Zou, Q.; Zeng, T.; Zhu, L. A Fluorescence-Phosphorescence-Phosphorescence Triple-Channel Emission Strategy for Full-Color Luminescence. *Small* **2020**, *16*, 1906475.

(28) Zhao, W.; He, Z.; Tang, B. Z. Room-Temperature Phosphorescence from Organic Aggregates. *Nat. Rev. Mater.* **2020**, *5*, 869-885.

(29) Mei, J.; Leung, N. L.; Kwok, R. T.; Lam, J. W.; Tang, B. Z. Aggregation-Induced Emission: Together We Shine, United We Soar! *Chem. Rev.* **2015**, *115*, 11718-11940.

(30) Tang, B. Z.; Zhao, Z.; Zhang, H.; Lam, J. W. Y. Aggregation-Induced Emission: New Vistas at Aggregate Level. *Angew. Chem. Int. Ed.* **2020**, *59*, 9888-9907.

(31) Ma, S.; Du, S.; Pan, G.; Dai, S.; Xu, B.; Tian, W. Organic Molecular Aggregates: From Aggregation Structure to Emission Property. *Aggregate* **2021**, *2*, e96.

(32) Shi, H.; Song, L.; Ma, H.; Sun, C.; Huang, K.; Lv, A.; Ye, W.; Wang, H.; Cai, S.; Yao, W.; Zhang, Y.; Zheng, R.; An, Z.; Huang, W. Highly Efficient Ultralong Organic Phosphorescence through Intramolecular-Space Heavy-Atom Effect. *J. Phys. Chem. Lett.* **2019**, *10*, 595-600.

(33) Ma, H.; Peng, Q.; An, Z.; Huang, W.; Shuai, Z. Efficient and Long-Lived Room-Temperature Organic Phosphorescence: Theoretical Descriptors for Molecular Designs. *J. Am. Chem. Soc.* **2019**, *141*, 1010-1015.

(34) Tsujimoto, H.; Ha, D. G.; Markopoulos, G.; Chae, H. S.; Baldo, M. A.; Swager, T. M. Thermally Activated Delayed Fluorescence and Aggregation Induced Emission with Through-Space Charge Transfer. *J. Am. Chem. Soc.* **2017**, *139*, 4894-4900.

(35) Yu, J.; Ma, H.; Huang, W.; Liang, Z.; Zhou, K.; Lv, A.; Li, X.-G.; He, Z. Purely Organic Room-Temperature Phosphorescence Endowing Fast Intersystem Crossing from Through-Space Spin-Orbit Coupling. *JACS Au* **2021**, *1*, 1694-1699.

(36) Shao, S.; Wang, L. Through-Space Charge Transfer Polymers for Solution-Processed Organic Light-Emitting Diodes. *Aggregate* **2020**, *1*, 45-56.

(37) Hua, C.; Doheny, P. W.; Ding, B.; Chan, B.; Yu, M.; Kepert, C. J.; D'Alessandro, D. M. Through-Space Intervalence Charge Transfer as a Mechanism for Charge Delocalization in Metal-Organic Frameworks. *J. Am. Chem. Soc.* **2018**, *140*, 6622-6630.

(38) Zhang, H.; Du, L.; Wang, L.; Liu, J.; Wan, Q.; Kwok, R. T. K.; Lam, J. W. Y.; Phillips, D. L.; Tang, B. Z. Visualization and Manipulation of Molecular Motion in the Solid State through Photoinduced Clusteroluminescence. *J. Phys. Chem. Lett.* **2019**, *10*, 7077-7085.

(39) Wang, H.; Li, Q.; Zhang, J.; Zhang, H.; Shu, Y.; Zhao, Z.; Jiang, W.; Du, L.; Phillips, D. L.; Lam,

J. W. Y.; Sung, H. H. Y.; Williams, I. D.; Lu, R.; Tang, B. Z. Visualization and Manipulation of Solid-State Molecular Motions in Cocrystallization Processes. *J. Am. Chem. Soc.* **2021**, *143*, 9468-9477.

(40) Leung, N. L.; Xie, N.; Yuan, W.; Liu, Y.; Wu, Q.; Peng, Q.; Miao, Q.; Lam, J. W.; Tang, B. Z. Restriction of Intramolecular Motions: The General Mechanism Behind Aggregation-Induced Emission. *Chem. Eur. J.* **2014**, *20*, 15349-15353.

(41) Zhang, J.; Zhang, H.; Lam, J. W. Y.; Tang, B. Z. Restriction of Intramolecular Motion (RIM): Investigating AIE Mechanism from Experimental and Theoretical Studies. *Chem. Res. Chin. Univ.* **2021**, *37*, 1-15.

(42) Tu, Y.; Zhao, Z.; Lam, J. W. Y.; Tang, B. Z. Mechanistic Connotations of Restriction of Intramolecular Motions (RIM). *Natl. Sci. Rev.* **2021**, *8*, nwaa260.

(43) Spackman, M. A.; Jayatilaka, D. Hirshfeld Surface Analysis. *CrystEngComm* **2009**, *11*, 19-32.